



**HAL**  
open science

# A multi-objective optimization problem in mixed and natural convection for a vertical channel asymmetrically heated

Delphine Ramalingom, Pierre-Henri Cocquet, Rezah Maleck, Alain Bastide

## ► To cite this version:

Delphine Ramalingom, Pierre-Henri Cocquet, Rezah Maleck, Alain Bastide. A multi-objective optimization problem in mixed and natural convection for a vertical channel asymmetrically heated. Structural and Multidisciplinary Optimization, 2019. hal-01620054v2

**HAL Id: hal-01620054**

**<https://hal.univ-reunion.fr/hal-01620054v2>**

Submitted on 30 May 2018 (v2), last revised 18 May 2020 (v4)

**HAL** is a multi-disciplinary open access archive for the deposit and dissemination of scientific research documents, whether they are published or not. The documents may come from teaching and research institutions in France or abroad, or from public or private research centers.

L'archive ouverte pluridisciplinaire **HAL**, est destinée au dépôt et à la diffusion de documents scientifiques de niveau recherche, publiés ou non, émanant des établissements d'enseignement et de recherche français ou étrangers, des laboratoires publics ou privés.

# A multi-objective optimization problem in natural convection for a vertical channel asymmetrically heated

Delphine Ramalingom<sup>a,\*</sup>, Pierre-Henri Cocquet<sup>a</sup>, Rezah Maleck<sup>a</sup>, Alain Bastide<sup>a</sup>

<sup>a</sup>*Université de La Réunion, Laboratoire PIMENT, 117 Avenue du Général Ailleret, 97430 Le Tampon, France*

---

## Abstract

This paper deals with a multi-objective topology optimization problem in an asymmetrically heated channel, considering both pressure drop minimization and heat transfer maximization. The problem is modeled under the assumptions of steady-state laminar flow dominated by natural convection forces. The incompressible Navier-Stokes equations coupled to the convection-diffusion equation through the Boussinesq approximation are employed and are solved with the finite volume method. In this paper, we propose two new objective functions: the first one takes into account work of pressure forces and contributes to the loss of mechanical power while the second one is related to thermal power and is linked to the maximization of heat exchanges. In order to obtain a well-defined fluid-solid interface in the optimized design, we use a sigmoid interpolation function for both the design variable field and the effective diffusivity. We also use adjoint sensitivity analysis to compute the gradient of the cost functional. Results are obtained for various Richardson (Ri) number such that  $100 < Ri < 400$  and

---

\*Corresponding author: delphine.ramalingom@univ-reunion.fr

for a Reynolds (Re) number set to  $Re = 400$ . In all considered cases, our algorithm succeeds to enhance one of the phenomenon modeled by our new cost functions without deteriorating the other one. We also show that the reversal flow is suppressed at the exit of the channel, the thermal exchanges are improved by our optimized designs. We also compare the results of standard cost functions from the literature to those of our cost functions. We show that the new objective functions reached stable values in less iteration number and allow best connectivity of solid elements. As a result the new objective functions proposed in this paper are well suited to deal with natural convection optimization problem.

*Keywords:* Natural convection, Vertical channel, Topology optimization, Objective functions, Adjoint sensitivity analysis, Sigmoid function

---

## Nomenclature

### List of abbreviations

$b$	Channel width
$d$	Width of circulation flow
$g$	Gravitational acceleration
$h_\tau$	Ratio between a kinematic viscosity and a permeability
$k_\tau$	Effective diffusivity, dimensionless
$p$	Pressure, dimensionless
$\mathbf{u}$	Velocity vector, dimensionless
$Gr_b$	Grashof number
$H$	Height of heated plate, channel height $A = 2H$
$Nu_2$	Nusselt number based on $\theta_b$
$Pr$	Prandtl number
$Q_t$	Proportion of material added in $\Omega$ at the end of optimization process
$Ra_b$	Rayleigh number based on $b$
$Re$	Reynolds number
$Ri$	Richardson number
$T$	Fluid temperature
$U$	Average velocity at the entrance of the channel

$\mathcal{J}$  Objective function

$\mathcal{L}$  Lagrangian function

### **Greek symbols**

$\alpha$  Design parameter

$\nu$  Kinematic viscosity

$\Phi$  Heat flux at the hot plate

$\Omega$  Computational domain

$\alpha_0, \tau$  Parameters of sigmoid functions

$\beta$  Thermal expansion coefficient

$\gamma_1, \gamma_2$  Weighting coefficients

$\Gamma$  Frontiers of the domain

$\Delta$  Variation

$\epsilon$  Stopping criterion in optimization algorithm

$\theta$  Temperature, dimensionless

$\lambda_f$  Thermal conductivity of fluid

### **Subscripts**

$b$  bulk

$o$  outlet

$i$  inlet

$max$  maximum value

## 1. Introduction

Topology optimization is a powerful and a popular tool for designers and engineers to design process. Its notion was initially introduced in structural mechanics by Bendsøe and Kikuchi [1]. In order to increase the structural stiffness under certain load, they targeted the optimal material density distribution by identifying areas in which material should be added. They expressed the design problem in terms of real valued continuous function per point, with values ranging from zero (indicating the presence of void/absence of material) to unity (indicating solid). The method has then been developed to numerous problems in structural mechanics [2, 3, 4, 5, 6, 7, 8]. In fluid mechanics, the same idea was adapted to Stokes flows by Borrvall and Petersson [9], by introducing a real-valued inverse permeability multiplied by a kinematic viscosity dependent term into the flow equations. Domain areas corresponding to the fluid flow are those where  $\alpha$  is equal to 0 while areas where  $\alpha$  is not equal to 0 define the part of the domain to be solidified. The optimal solid walls to be designed correspond to the interfaces between the two aforementioned areas. So, the goal of topology optimization is to compute the optimal  $\alpha$  field in order to minimize some objective function under consideration. Contrary to topology optimization applied to design structure, research on topology optimization applied to heat transfer and fluid dynamics is quite recent. Dbouk [10] presented a review about topology optimization design methods that have been developed for heat transfer systems, and for each of them, he presented their advantages, limitations and perspectives. In topology optimization problems with large number of design variables, gradient-based algorithms are frequently used to compute accurate solutions

26 efficiently [11, 12, 13, 14, 15, 16]. This algorithm starts with a given geometry  
27 and iterates with information related to the derivatives (sensitivity deriva-  
28 tives) of the objective function with respect to the design variables. Among  
29 the methods used to compute the sensitivity derivatives required by gradient-  
30 based methods, the adjoint method [11, 17, 18, 19, 12, 20] has been receiving  
31 a lot of attention since the cost of computing the necessary derivatives is  
32 independent from the number of design variables. Papoutsis-Kiachagias and  
33 Giannakoglou [18] present a review on continuous adjoint method applied  
34 to topology optimization for turbulent flows. Tong et al. [21] have recently  
35 discussed on the optimization of thermal conductivity distribution for heat  
36 conduction enhancement. They considered different optimization objectives  
37 and demonstrate that they should be carefully chosen when heat conduction  
38 is involved. Othmer [19] derived the continuous adjoint formulations and the  
39 boundary conditions on ducted flows for typical cost functions. He proposed  
40 an objective function to reduce pressure drops in open cavity. The origi-  
41 nality of his method is the versatility of the formulation where the adjoint  
42 boundary conditions were expressed in a form that can be adapted to any  
43 commonly used objective function. Then, for the automotive industry, Oth-  
44 mer et al. [22] implemented several objective functions like dissipated power,  
45 equal mass flow through different outlets and flow uniformity. To describe  
46 the transition and interface between fluid and solid regions in the domain,  
47 the Solid Isotropic Material with Penalization (SIMP) technique [1, 23] is  
48 the mostly used in the literature as the interpolation technique in topology  
49 optimization. This approach represents the non-fluid regions as infinitely  
50 stiff, a penalty to the flow, such that no interaction is modeled. Yoon [16]

51 presented a method for solving static fluid-structure interaction problems by  
52 converting the stresses at the fluid-solid interfaces into a volume integral rep-  
53 resentation. A new method of interpolation was presented by Ramalingom  
54 et al. [24] in order to improve the interface fluid-solid during the optimiza-  
55 tion process. They proposed two sigmoid functions to interpolate material  
56 distribution and effective diffusivity. They showed that transition zones, i.e.  
57 zones where the velocity of fluid is too large to be considered as solid, can  
58 be made arbitrary small.

59 Convection typically is categorized, according to fluid motion origins, as  
60 forced, mixed or natural [25, 26]. All aforementioned references on heat  
61 transfer problems deal with forced or mixed convection. This means that  
62 the fluid motion is driven by a fan, pump or pressure gradient often modeled  
63 by a non-null velocity at entrance of the studied domain. Although nat-  
64 ural convection is often used for the passive cooling of industrial systems,  
65 very few studies have been investigated for topology optimization problem  
66 in natural convection case. Natural convection involves a heat dissipation  
67 mechanism where the fluid motion is governed by differences in buoyancy  
68 arising from temperature gradients. More precisely, the fluid is submitted  
69 to a small velocity, the corresponding heat rates are also much lower than  
70 those associated with forced convection. Coffin and Maute [27] introduced  
71 a topology optimization method for 2D and 3D, steady-state and transient  
72 heat transfer problems that are dominated by natural convection in the fluid  
73 phase. The geometry of the fluid-solid interface is described by an explicit  
74 level set method. Alexandersen et al. [13] applied topology optimization to  
75 natural convection problems. Its study shows that topology optimization is

76 a viable approach for designing heat sink geometries cooled by natural con-  
77 vection and micropumps powered by natural convection. He treated several  
78 difficulties that would be encountered when dealing with natural convection  
79 problems as the oscillatory behavior of the solver, namely a damped Newton  
80 method, used for the optimization computations. He also reported intermedi-  
81 ate relative densities that amplified the natural convection effects leading to  
82 non-vanishing velocity in some solid parts of the computational domain. As a  
83 result, those zones are considered as solid by the optimization algorithm while  
84 they should be treated as fluid. Bruns [15] applied topology optimization to  
85 convection-dominated heat transfer problems. He highlighted numerical in-  
86 stabilities in convection-dominated diffusion problems and justified them by  
87 the density-design-variable-based topology optimization.

88 Other numerical issues are encountered in topology optimization prob-  
89 lems, as checkerboards pattern and intermediate density regions. Authors  
90 usually adopted a continuation strategy where the parameter involved in the  
91 SIMP interpolation of the effective diffusivity is gradually increased during  
92 the optimization process. These values are chosen to aggressively penalize  
93 intermediate densities with respect to effective diffusivity and to confine the  
94 maximum impermeability to the fully solid parts of the domain. Similarly,  
95 authors used filtering techniques [28, 29, 30, 12, 13] to overcome checker-  
96 boards. The filtering is done by looking at the "neighborhood" of the indi-  
97 vidual element which is defined as the set of elements with centers within the  
98 filter radius. Bruns [29] explained that the main disadvantage of filtering the  
99 sensitivities is that the approach is heuristic because the sensitivities are not  
100 consistent with the primal analysis. Therefore, the optimization problem is

101 not well posed in a rigorous sense. Alexandersen et al. [31] explained that  
102 some form of filtering can be beneficial for some topology optimization prob-  
103 lems. Minimizing the dissipate energy in fluid flow problems are generally  
104 well posed and no filtering is needed. In contrarily, alternating solid and  
105 fluid elements can exist in structural and heat transfer problems. That cre-  
106 ates areas of solid elements not correctly connected. Sigmund [32] described  
107 various filters type to fix this problem.

108 In this paper, we deal with some topology optimization problems for heat  
109 and mass transfers, considering the physical case of an asymmetrically heated  
110 vertical channel. This geometry has been subject to numerous studies in the  
111 literature [33, 34, 35, 36]. The first investigations date back to 1942 with the  
112 works of Martinelli and Boelter [37] according to the comprehensive review  
113 of Jackson et al. [38]. Developing and fully developed laminar free convection  
114 within heated vertical plates were subsequently investigated numerically by  
115 Bodoia and Osterle [39] and was experienced by Elenbaas [40]. Since then,  
116 many studies were carried out. This great interest can be explained by  
117 the fact that this configuration is encountered in several industrial devices  
118 such as solar chimney, energy collectors, electronic components and even in  
119 nuclear reactors. The optimization of these systems simultaneously demands  
120 compactness, efficiency and control of heat and mass transfers.

121 This paper investigates new objective functions to optimize heat transfer  
122 in convection-dominated diffusion problems. Instead of proposing methods  
123 to improve filtering techniques and avoid some non-physical solutions re-  
124 lated in literature [41, 15], we propose new expressions of objective functions  
125 within the framework of topology optimization applied to an asymmetrically

126 heated vertical channel. Furthermore, no filtering techniques have been used  
127 during the optimization process. The geometry considered here is the model  
128 proposed by Desrayaud et al. [42] and corresponds to a boundary layer flow  
129 with a reversal flow at the exit [43]. We study the influence of Richardson  
130 number, which represents the importance of natural convection relative to  
131 the forced convection, in the optimized design. This adimensional number  
132 is chosen such as natural convection forces are dominant. Our optimization  
133 algorithm succeeds especially to suppress the reversal flow. We show that our  
134 optimized design increase thermal exchanges by computing the Nusselt num-  
135 bers for the range of Richardson numbers considered. We finally compare our  
136 results at the end of the optimization process to those obtained with classical  
137 objective functions of the literature. We conclude that our expression of cost  
138 functions are best suited to the optimization of convection-dominated diffu-  
139 sion problems which agrees closely with Tong et al. [21] about the importance  
140 of the choice of objective function in optimization problem.

## 141 **2. Governing equations**

142 The flows considered in this paper are assumed to be in a steady-state  
143 laminar regime, newtonian and incompressible. Figure 1 shows the configu-  
144 ration of the computational domain  $\Omega$ .

145 Physical properties of the fluid are kinematic viscosity  $\nu$  and thermal  
146 conductivity  $\lambda_f$ . First, parameters governing the flow is the Reynolds number  
147 defined as  $\text{Re} = U b/\nu$ , with  $b$  being the width of the channel and  $U$  the  
148 reference velocity based on the average velocity at the channel entrance. The  
149 Prandtl number is defined as  $\text{Pr} = \nu/k$ . It describes the ratio between the

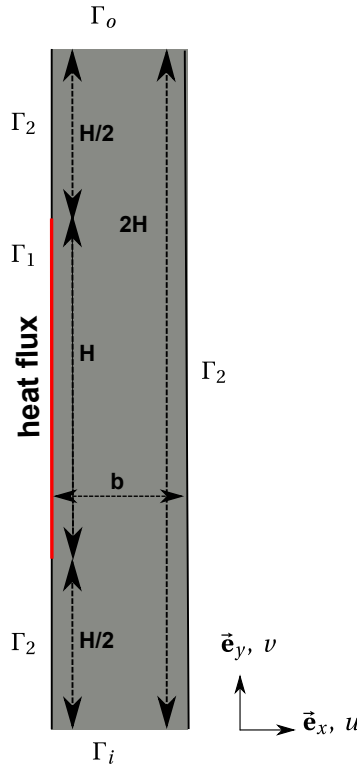


Figure 1: Geometry of the problem

150 momentum and thermal diffusivities of the fluid. In this paper, we consider  
 151 only fluids with small Prandtl as  $\text{Pr} < 1$ . The Grashof number is defined as  
 152  $\text{Gr}_b = g \beta \Delta T b^3 / \nu^2$  and represents the ratio between buoyancy and viscous  
 153 force.  $\Delta T = -\phi / \lambda_f$ ,  $\phi$  is the thermal flux on  $\Gamma_1$ . In thermal convection  
 154 problems, Richardson number  $\text{Ri} = \text{Gr}_b / \text{Re}^2$  represents the importance of  
 155 natural convection relative to the forced convection. For values greater than  
 156 unity, we know that the flow is dominated by natural convection. Under these  
 157 assumptions and thanks to a method given in Borrvall and Petersson [9], the  
 158 porosity field is introduced in the steady-state Navier-Stokes equation as a  
 159 source term  $h_\tau(\alpha)\mathbf{u}$  which yields a Brinkman-like model with a convection

160 term [24]. Therefore, the dimensionless form of the Navier-Stokes and energy  
 161 equations are written as follows:

$$\begin{aligned}
 \nabla \cdot \mathbf{u} &= 0 && \text{in } \Omega, \\
 (\mathbf{u} \cdot \nabla) \mathbf{u} &= -\nabla p + \text{Re}^{-1} \Delta \mathbf{u} - h_\tau(\alpha) \mathbf{u} + \text{Ri } \theta \vec{e}_y && \text{in } \Omega, \\
 \nabla \cdot (\mathbf{u} \theta) &= \nabla \cdot (\text{Re}^{-1} \text{Pr}^{-1} k_\tau(\alpha) \nabla \theta) && \text{in } \Omega,
 \end{aligned} \tag{1}$$

163 where  $(\mathbf{u}, p, \theta)$  correspond respectively to dimensionless velocity, pressure and  
 164 temperature and are usually referred as the primal variable in the current set-  
 165 ting. Parameter  $\alpha$  is the spatially varying design variable field determined by  
 166 the optimization algorithm. For the natural-dominated convection problem,  
 167 we consider the following boundary conditions:

$$\begin{aligned}
 \mathbf{u} &= 0, \quad \nabla p = 0, \quad \partial_n \theta = -1 && \text{on } \Gamma_1, \\
 \mathbf{u} &= 0, \quad \nabla p = 0, \quad \partial_n \theta = 0 && \text{on } \Gamma_2, \\
 \mathbf{u} &= u_i \mathbf{e}_y, \quad \nabla p = 0, \quad \theta = 0 && \text{on } \Gamma_i, \\
 \partial_n \mathbf{u} &= 0, \quad p = 0, \quad \partial_n \theta = 0 && \text{on } \Gamma_o,
 \end{aligned} \tag{2}$$

169 where  $\partial_n$  is the normal derivative defined as  $\partial_n = n \cdot \nabla$ .

### 170 3. Topology optimization formulation

171 The main goal of this paper is to deal with a multi-objective optimization  
 172 problem in the asymmetrically heated channel, considering both pressure  
 173 drop minimization described by a first objective function  $\mathcal{J}_1$  and heat transfer  
 174 maximization described by a second objective function  $\mathcal{J}_2$ . The optimization

175 problem can then be stated as:

$$\begin{aligned} &\text{minimize: } \mathcal{J}(\mathbf{u}, p, \theta) = \gamma_1 \mathcal{J}_1(\mathbf{u}, p, \theta) + \gamma_2 \mathcal{J}_2(\mathbf{u}, p, \theta), \\ &\text{subject to: } \text{Governing equations (1),} \\ &\quad \text{Boundary conditions (2).} \end{aligned} \tag{3}$$

177 where the cost function  $\mathcal{J}$  is the combination of the two objectives functions,  
178  $\gamma_1$  and  $\gamma_2$  are weighting coefficients. It is easy to observe that, for  $\gamma_1 \gg \gamma_2$ , the  
179 multi-objective function is directed to a minimum power dissipation problem,  
180 while for  $\gamma_1 \ll \gamma_2$ , a maximum heat dissipation problem arises.

### 181 3.1. Definition of the cost functions

182 As indicated by several authors [30, 12, 17, 14], cost functions  $\mathcal{J}_1$  and  $\mathcal{J}_2$   
183 are often expressions of the work of forces or powers that one either wish  
184 to minimize or to maximize. A classical cost function used by Marck et al.  
185 [12], Othmer [19] for evaluating total pressure losses is :

$$186 \quad f(\mathbf{u}, p) = \int_{\Gamma} -\mathbf{n} \cdot \mathbf{u} \left( p + \frac{1}{2} |\mathbf{u}|^2 \right) dS. \tag{4}$$

187 Also, Marck et al. [12], Kontoleon et al. [17] evaluate the thermal power  
188 by the next expression:

$$189 \quad f(\mathbf{u}, \theta) = \int_{\Gamma} \mathbf{n} \cdot \mathbf{u} \theta dS. \tag{5}$$

190 In our study, we propose to evaluate mechanical power and thermal power  
191 via two new expressions of both cost functions. As we will show below,  
192 these functions give an optimal design in less iteration number and do not  
193 require the use of filtering techniques. They will also allow to obtain a good  
194 connectivity between elements of solid regions. For a system with an inlet,

195 an outlet, an average velocity and an average temperature, we define the  
 196 thermal power as the product of the mass flow, the volume heat capacity  
 197 and the difference of temperature between the entrance and the exit of the  
 198 system. Likewise, mechanical power is defined as the product of mass flow  
 199 rate and the difference of total pressure between the entrance and the exit  
 200 of the system. In that way, we chose the work of pressure forces to minimize  
 201 the power dissipated in the channel as used in systemic approach. Hence,  
 202 the first cost function can be written as:

$$\begin{aligned}
 \mathcal{J}_1(\mathbf{u}, p) = & -\frac{1}{|\Gamma_i|} \int_{\Gamma_i} p_t \, dS \int_{\Gamma_i} \mathbf{u} \cdot \mathbf{n} \, dS \\
 & -\frac{1}{|\Gamma_o|} \int_{\Gamma_o} p_t \, dS \int_{\Gamma_o} \mathbf{u} \cdot \mathbf{n} \, dS,
 \end{aligned} \tag{6}$$

204 where  $p_t = p + 1/2 |\mathbf{u}|^2$  is the total pressure,  $\Gamma_i$  and  $\Gamma_o$  are respectively the  
 205 entrance (inlet) and the exit (outlet) of the channel.

206 The second cost function concerns thermal exchange maximization and  
 207 is given by:

$$\begin{aligned}
 \mathcal{J}_2(\mathbf{u}, \theta) = & \frac{1}{|\Gamma_i|} \int_{\Gamma_i} \theta \, dS \int_{\Gamma_i} \mathbf{u} \cdot \mathbf{n} \, dS \\
 & + \frac{1}{|\Gamma_o|} \int_{\Gamma_o} \theta \, dS \int_{\Gamma_o} \mathbf{u} \cdot \mathbf{n} \, dS.
 \end{aligned} \tag{7}$$

209 We can observe that this systemic approach for defining our cost functions  
 210 enables to dissociate total pressure or temperature from the mass flow rate,  
 211 since velocity profile is imposed at the entrance. Besides, minimizing (Eq.  
 212 7) is equivalent to minimize the mean temperature at apertures. On the  
 213 contrary, minimizing (Eq. 5) is equivalent to minimize the bulk temperature  
 214 which is defined as:

$$\theta_b = \frac{1}{\int_{\Gamma_i} \mathbf{u} \cdot \mathbf{n} \, d\Gamma} \int_{\Gamma_i} \theta \, \mathbf{u} \cdot \mathbf{n} \, d\Gamma. \tag{8}$$

216 One can finally remark that, our expression of thermal power consists in the  
 217 mean temperature whereas expressions used by Marck et al. [12], Kontoleon-  
 218 tos et al. [17] corresponds to the bulk temperature.

### 219 3.2. Multi-objective optimization

220 In multi-objective optimization, the challenge is to benefit from both ob-  
 221 jective functions. As introduced in previous subsection, the objective func-  
 222 tion based on maximization of thermal exchanges can involve the increase of  
 223 pressure drop and conversely for the objective function relative to the dissi-  
 224 pation of power. Before combining linearly the two functions, they must then  
 225 be rescaled to have the same order of magnitude. This can be done by using  
 226 an Aggregate Objective Function (AOF), also known as the weighted-sum  
 227 approach, which is based on a linear combination of both objective functions  
 228 [44, 45]. The latter reads:

$$229 \quad \hat{f} = \frac{f - f_{min}}{f_{max} - f_{min}} \quad (9)$$

230 where  $f$  is either  $\mathcal{J}_1$  or  $\mathcal{J}_2$ . As explained by Marck et al. [12], the other four  
 231 parameters are determined by solving both optimization problems indepen-  
 232 dently (3) for  $\min \mathcal{J}_1$  and  $\max \mathcal{J}_2$ . Consequently, both rescaled objective  
 233 functions are ranged between 0 and 1. Such a rescaling allows to consider  
 234 the following linear combination:

$$235 \quad \hat{\mathcal{J}} = \omega \hat{\mathcal{J}}_1 - (1 - \omega) \hat{\mathcal{J}}_2 \quad (10)$$

236 where  $\omega \in [0, 1]$  is the weight balancing the influence of each objective func-  
 237 tion. Note that this combination involves the opposite of  $\mathcal{J}_2$  since one aims  
 238 at minimizing the combinatory function  $\hat{\mathcal{J}}$ . Thereafter,  $\hat{\mathcal{J}}_1$  and  $\hat{\mathcal{J}}_2$  are used  
 239 only during the optimization process.

## 240 4. Topology optimization methods

241 Applying topology optimization to this problem aims to minimize an  
242 objective function  $\mathcal{J}$  by finding an optimal distribution of solid and fluid  
243 element in the computational domain. The goal of topology optimization is  
244 to end up with binary designs, i.e avoid that the design variables take other  
245 value than those representing the fluid or the solid. This is usually carried  
246 out by penalizing the intermediate densities with respect to the material  
247 parameters, such as inverse permeability and effective diffusivity. A standard  
248 approach is to use interpolation functions. We are also going to use gradient-  
249 based algorithm that relies on the continuous adjoint method.

### 250 4.1. Interpolation functions

251 The additional term  $h_\tau(\alpha)$  in (Eq. 1) physically corresponds to the ratio  
252 of a kinematic viscosity and a permeability. As proposed by Guest et al.  
253 [46], Sigmund [32], Zhao et al. [47], a projection approach is employed to  
254 relate the element-based design variables to the physical densities firstly and  
255 to the thermal diffusivity, secondly. We defined two smooth regularization of  
256 Heaviside functions for these interpolations. The interpolation function for  
257 the thermal diffusivity of each element is  $k_\tau(\alpha)$ , both functions were defined  
258 in Ramalingom et al. [24] where it is shown that the intermediate zones can  
259 be as small as wanted. Regions with very high permeability can be considered  
260 as solid regions, and those with low permeability regions are interpreted as  
261 pure fluid.

262 Inverse permeability is thus interpolated with the following formula

$$263 \quad h_\tau(\alpha) = \alpha_{max} \left( \frac{1}{1 + \exp(-\tau(\alpha - \alpha_0))} - \frac{1}{1 + \exp(\tau\alpha_0)} \right), \quad (11)$$

264 where  $\alpha_0$  is the abscissa slope of the sigmoid function,  $\alpha_{max}$  is the maximum  
 265 value that the design parameter  $\alpha$  can take and is set to  $2 \cdot 10^5$ . In the present  
 266 study, we chose  $\alpha_0 = 20$  and  $\alpha \in [0, \alpha_{max}]$ .

267 The difference in the adimensional thermal diffusivities of the fluid and  
 268 solid regions is considered through the interpolation of effective diffusivity  
 269  $k_\tau$  as follows:

$$270 \quad k_\tau(\alpha) = \frac{1}{k_f} \left[ k_f + (k_s - k_f) \left( \frac{1}{1 + \exp(-\tau(\alpha - \alpha_0))} - \frac{1}{1 + \exp(\tau\alpha_0)} \right) \right], \quad (12)$$

271 where  $k_s$  and  $k_f$  are respectively the thermal diffusivity of solid domains and  
 272 the thermal diffusivity of the fluid domains.

#### 273 4.2. Adjoint problem

274 The Lagrange multiplier method [48] is used to get an optimization prob-  
 275 lem without constraints and can be used to get the sensitivity of the cost  
 276 function  $\mathcal{J}$ . The Lagrangian is defined as

$$277 \quad \begin{aligned} \mathcal{L}(\mathbf{u}, p, \theta, \mathbf{u}^*, p^*, \theta^*, \alpha) &= \mathcal{J}(\mathbf{u}, p, \theta) \\ &+ \int_\Omega \mathcal{R}(\mathbf{u}, p, \theta) \cdot (\mathbf{u}^*, p^*, \theta^*) d\Omega, \end{aligned} \quad (13)$$

278 where  $(\mathbf{u}^*, p^*, \theta^*)$  are the adjoint variables and  $\mathcal{R}(\mathbf{u}, p, \theta) = 0$  corresponds  
 279 to the governing equations (1). The critical points of  $\mathcal{L}$  with respect to the  
 280 adjoint variables give the constraint of the optimization problem (3) while the  
 281 critical point with respect to the primal variable yield the so-called adjoint

282 problem. The latter can be derived as in Othmer [19] (see also [24]) and is  
 283 given by

$$\begin{aligned}
 \nabla p^* - h_\tau(\alpha) \mathbf{u}^* + \theta \nabla \theta^* + Re^{-1} \Delta \mathbf{u}^* + \nabla \mathbf{u}^* \cdot \mathbf{u} - (\mathbf{u}^* \cdot \nabla) \mathbf{u} &= 0 \quad \text{in } \Omega, \\
 \nabla \cdot \mathbf{u}^* &= 0 \quad \text{in } \Omega, \\
 Ri \mathbf{u}^* \cdot \vec{e}_y + \mathbf{u} \cdot \nabla \theta^* + \nabla \cdot (Re^{-1} Pr^{-1} k_\tau(\alpha) \nabla \theta^*) &= 0 \quad \text{in } \Omega,
 \end{aligned} \tag{14}$$

284

285 together with the boundary conditions

$$\begin{aligned}
 \mathbf{u}^* = 0, \quad \partial_n \theta^* = 0, \quad \partial_n p^* = 0 & \quad \text{on } \Gamma_1 \cup \Gamma_2, \\
 u_i^* = 0, \quad \theta^* = 0, \quad \frac{\partial \mathcal{J}}{\partial p} = -u_n^*, \quad \partial_n p^* = 0 & \quad \text{on } \Gamma_i, \\
 u_i^* = 0, \quad \frac{\partial \mathcal{J}}{\partial \theta} = -\theta^* u_n - Re^{-1} Pr^{-1} k_\tau(\alpha) \partial_n \theta^* & \quad \text{on } \Gamma_o, \\
 \frac{\partial \mathcal{J}}{\partial \mathbf{u}} \cdot \mathbf{n} = -p^* - \theta^* \theta - Re^{-1} \partial_n \mathbf{u}^* \cdot \mathbf{n} - u_n^* u_n - \mathbf{u} \cdot \mathbf{u}^* & \quad \text{on } \Gamma_o,
 \end{aligned} \tag{15}$$

286

287 where  $u_n = \mathbf{u} \cdot \mathbf{n}$  and the derivatives of  $\mathcal{J}$  defined in (3) with respect to  
 288  $(\mathbf{u}, p, \theta)$  are given by

$$\begin{aligned}
 \left. \frac{\partial \mathcal{J}}{\partial p} \right|_{\Gamma_i} &= -\gamma_1 \frac{1}{|\Gamma_i|} \int_{\Gamma_i} \mathbf{u} \cdot \mathbf{n} \, dS \\
 \left. \frac{\partial \mathcal{J}}{\partial \theta} \right|_{\Gamma_o} &= \gamma_2 \frac{1}{|\Gamma_o|} \int_{\Gamma_o} \mathbf{u} \cdot \mathbf{n} \, dS \\
 \left. \frac{\partial \mathcal{J}}{\partial \mathbf{u}} \right|_{\Gamma_o} &= -\gamma_1 \frac{1}{|\Gamma_o|} \mathbf{n} \int_{\Gamma_o} p_t \, dS - \gamma_1 \mathbf{u} \cdot \int_{\Gamma_o} \mathbf{u} \cdot \mathbf{n} \, dS \\
 &+ \gamma_2 \frac{1}{|\Gamma_o|} \mathbf{n} \int_{\Gamma_o} \theta \, dS.
 \end{aligned} \tag{16}$$

289

290 We emphasize that the adjoint problem (14,15) has been derived for the  
 291 cost function  $\mathcal{J}$  given by (3). Nevertheless, in the numerical result, we wish  
 292 to minimize the rescaled cost function  $\hat{\mathcal{J}}$  whose derivatives with respect to

293  $(\mathbf{u}, p, \theta)$  are obtained thanks to (16) with

$$294 \quad \gamma_1 = \frac{\omega}{\mathcal{J}_{1,max} - \mathcal{J}_{1,min}}, \quad \gamma_2 = \frac{-(1 - \omega)}{\mathcal{J}_{2,max} - \mathcal{J}_{2,min}}.$$

### 295 4.3. Implementation

296 Topology optimization problem is solved by iterative calculations as car-  
 297 ried out by Ramalingom et al. [24]. The main steps of the algorithm for the  
 298 topology optimization are summarized in Table 2. They consist to compute  
 299 sensitivities by adjoint method and evaluate the optimality condition. If a  
 300 stopping criterion is met, the computations are terminated. For our simula-  
 301 tions, we used  $\epsilon = 10^{-7}$ . The forward problem (1) and the adjoint problem  
 302 (14) are implemented using OpenFOAM [49]. The generalized Geometric-  
 303 Algebraic Multi-Grid (GAMG) solver with a cell-centered colocalized finite  
 304 volume approach is used. In Step 5, the design variables are evaluated by  
 305 using the conjugated-gradient descent direction method associated to Polack-  
 306 Ribiere method  $\beta_{k+1}^{PR} = \frac{\nabla \mathcal{J}_{k+1}^T (\nabla \mathcal{J}_{k+1} - \nabla \mathcal{J}_k)}{\nabla \mathcal{J}_k^T \nabla \mathcal{J}_k}$ . The optimality condition is given  
 307 by the critical point of the Lagrangian with respect to the design parameter  
 308  $\alpha$  as follows:

$$309 \quad \frac{\partial h_\tau}{\partial \alpha} \mathbf{u} \cdot \mathbf{u}^* + \frac{\partial k_\tau}{\partial \alpha} \nabla \theta \cdot \nabla \theta^* = 0 \quad \text{in } \Omega, \tag{17}$$

$$310 \quad \frac{\partial k_\tau}{\partial \alpha} \theta^* = 0 \quad \text{with } \partial_n \theta = -1 \quad \text{on } \Gamma_1.$$

## 311 5. Results

312 First of all, it is important to note that the problem is purely academic and  
 313 the values of various parameters as Prandtl number set to 0.71 corresponding

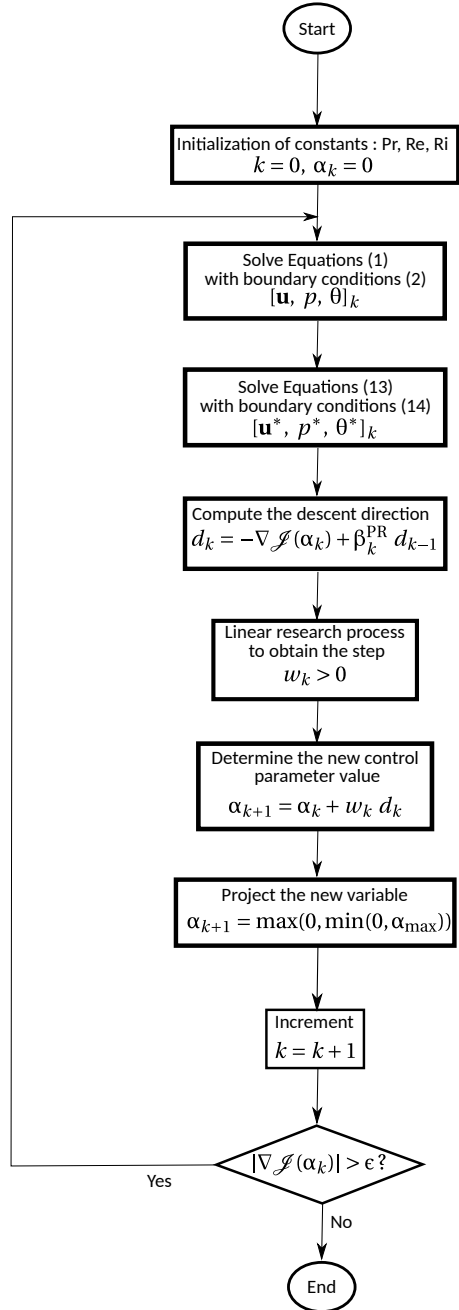


Figure 2: Algorithm used to solve the topology optimization (3)

314 to a fluid/liquid, and  $k_s/k_f$  have been therefore set to 3. As they are in  
 315 the range of realistic problems, they are thought to be representative of the  
 316 problems that can be physically encountered. The problem is investigated for  
 317  $Ri = \{100, 200, 400\}$  under constant  $Re = 400$  which is equivalent to increase  
 318 the dominance of natural convection in the conducto-convection problem.  
 319 These values have been chosen in accordance with the study of Li et al. [50]  
 320 on reversal flows in the asymmetrically heated channel. We chose  $\alpha_0 = 20$   
 321 and set  $\alpha_{max}$  to  $2 \cdot 10^5$ , keeping in mind that similar results have been  
 322 obtained for  $\alpha_{max} = 10^6$ . A vertical velocity profile at the entrance of the  
 323 channel is considered in accordance with the value of  $Re = 400$ . Its profile is  
 324 defined by the following equation:

$$325 \quad u_i(x) = - 6.1 x^2 + 6.1 x.$$

326 For this study, we chose different values of  $\omega$  in line with the importance  
 327 given to the different cost functions  $\mathcal{J}_1$  or  $\mathcal{J}_2$ . All results performed in this  
 328 paper correspond to the thermal and mechanical powers defined as  $\mathcal{J}_1$  and  
 329  $\mathcal{J}_2$ . Moreover, in order to be sure that no material is added at the entrance  
 330 of the channel during the optimization process, we solved the problem by  
 331 imposing fluid domain at the lower part of the channel, i.e.  $\alpha = 0$  for the  
 332 element in  $[0, 1] \times [0, 1]$ . We compare first the various optimized designs  
 333 obtained and the structure of the flow in new designs. For each value of  
 334 Richardson number, we compute the proportion  $Q_t$  of material added in the  
 335 domain  $\Omega$  as follows:

$$336 \quad Q_t = \frac{\int_{\Omega} h_{\tau}(\alpha) d\Omega}{\alpha_{max} V_{tot}}, \text{ where } V_{tot} \text{ is the total volume of } \Omega. \quad (18)$$

337 In order to demonstrate the increase of heat transfer after optimization, we

338 compute the inverse of the difference between the temperature at the left  
 339 wall and the bulk temperature, i.e the Nusselt number defined in Desrayaud  
 340 et al. [42] by:

$$Nu_2(y) = \frac{1}{\theta(0, y) - \theta_{bulk}(y)} \quad (19)$$

$$\text{where } \theta_{bulk}(y) = \frac{1}{q_{in}(y=0)} \int_0^1 u(x, y) \theta(x, y) dx,$$

342  $y = 3H/2$  corresponds to the end of the heated plate and  $q_{in}$  is the mass flow  
 343 rate entering the channel at  $y = 0$ .

344 In a second time, we compare our results obtained for  $Ri=100$  to those  
 345 obtained with objectives function usually used in literature, i.e.  $\mathcal{J}_1$  and  $\mathcal{J}_2$   
 346 are defined by (Eq. 4) and (Eq. 5).

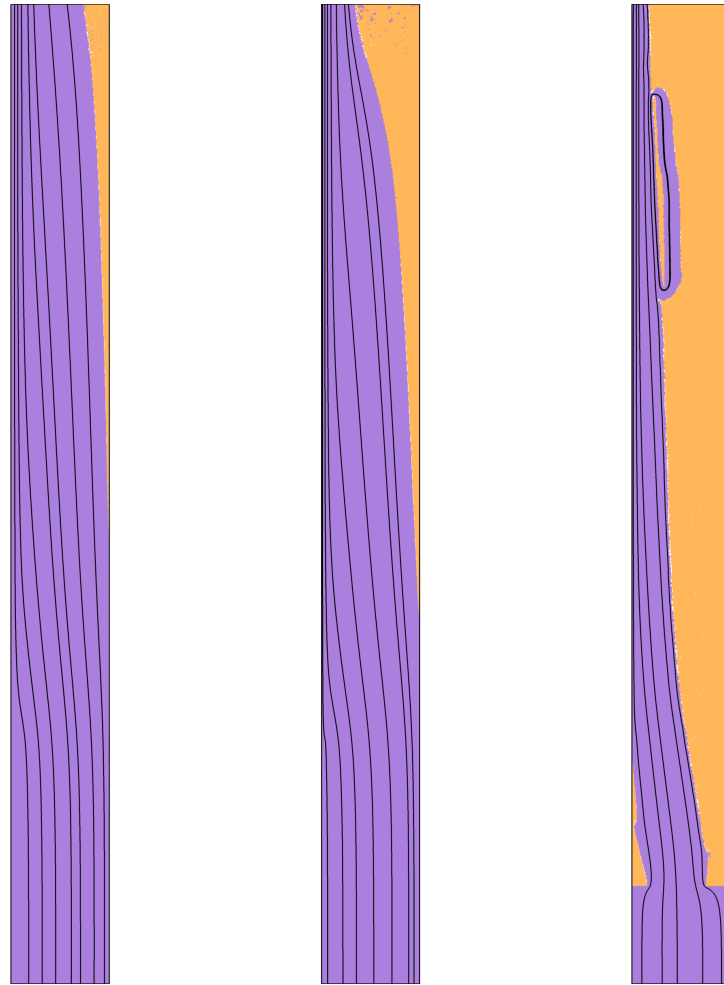
### 347 5.1. Varying Richardson number

348 Figure 3 shows that the obtained designs at varying  $Ri$  differ from one  
 349 to another, which is to be expected. When the natural convection forces  
 350 become more dominant, the optimization algorithm adds more material in  
 351 the channel. The proportion of material added in the vertical channel varies  
 352 from 4.9% to 52.2%. So, the quantity of material increases when Richardson  
 353 number increases. The structure of the flow in the channel is also modified.  
 354 From Figure 3c, it can be seen that for  $Ri = 400$ , all of the material is kept  
 355 close to the right wall of the domain and the flow circulation is obliged to  
 356 be near the heated wall. This contributes to the second objective function  
 357 corresponding to increase the thermal exchanges in the channel. Table 1  
 358 gives the Nusselt number at the exit of the heated plate for each Richardson

359 number. Without optimization and whichever the Richardson number in the  
360 range considered, Nusselt number at the exit of hot plate is equal to 10.51  
361 and the bulk temperature to 0.07. After optimization, Nusselt number varies  
362 from 11.86 to 15.06. Hence, we obtained a rise between 12.8% and 43.3%. So,  
363 Nusselt number is more important in the optimized design and it increases  
364 when Richardson number increases. Hence, we successfully increase thermal  
365 exchanges in the channel.

366 It can also be observed that the reversal flow is suppressed after opti-  
367 mization process. Indeed, material added by the algorithm at the end of the  
368 channel prevent the fluid from re-entering in the channel. As can be seen  
369 on Figure 5, vertical component of the velocity has a positive value in the  
370 channel after optimization and is null or very small in the solid region, as  
371 expected. That means our interpolation function gives an optimized design  
372 with no physical error as a non-null velocity in the solid regions without con-  
373 nectivity (Kreissl and Maute [51] and Lee [30]). Moreover, value of vertical  
374 component of the velocity increases when  $Ri$  increases (cf. Figure 4). That  
375 is due to the reduction of the section for the flow circulation which causes an  
376 acceleration of the fluid in the channel. The width of flow circulation after  
377 optimization for the case  $Ri = 100, \omega = 0.5$  is referenced on Figure 6, for ex-  
378 ample. This graph also demonstrates that the sigmoid function  $h_\tau(\alpha)$  which  
379 interpolates the design variable  $\alpha$  affects correctly volume elements to solid  
380 domains in order to avoid checkerboards. That brings to a well definition of  
381 the fluid-solid boundaries as obtained by Ramalingom et al. [24].

382 With regards of cost functions computation, our algorithm reduces the  
383 value of  $\tilde{J}$  over iterations as can be seen on Figure 7 for the case  $Ri = 100$ .



(a)  $Ri = 100$   
 $Q_t = 4.9\%$

(b)  $Ri = 200$   
 $Q_t = 13.3\%$

(c)  $Ri = 400$   
 $Q_t = 52.2\%$

Figure 3: Optimized designs and streamtraces at various  $Ri$ . Orange corresponds to solid material and purple corresponds to the fluid domain.

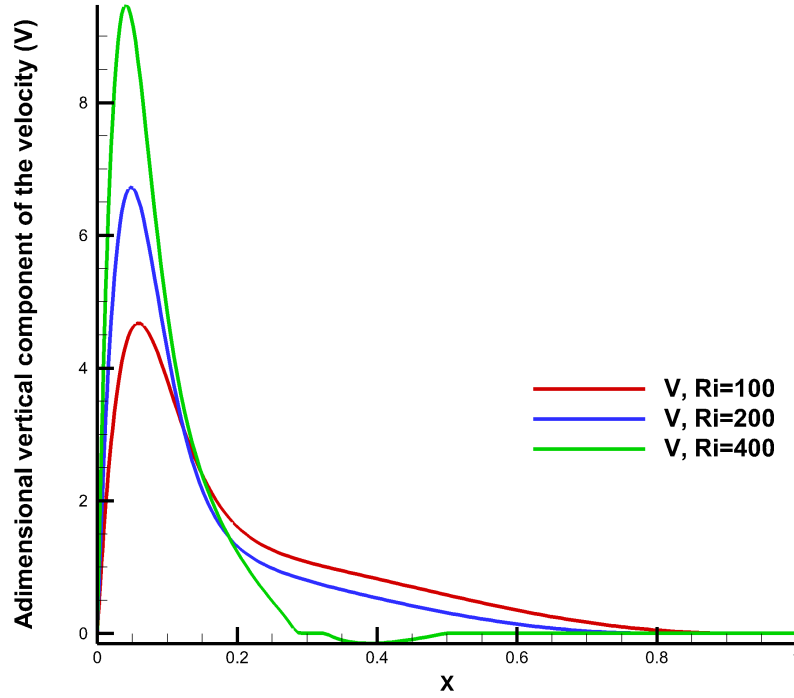
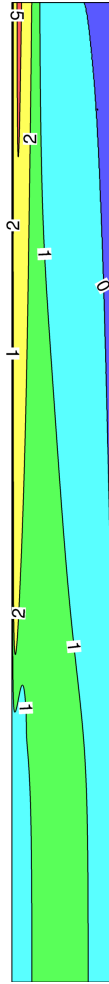
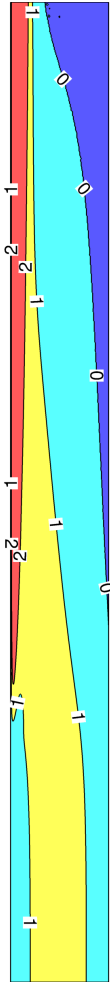


Figure 4: Adimensional vertical component of the velocity at the end of the hot plate of the channel  $y = 3H/2$

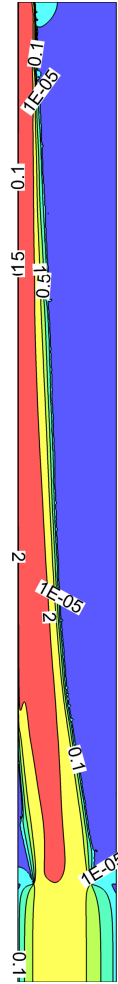
384 Table 2 highlights the influence of Ri on thermal power and mechanical power.  
 385 Indeed, as the Richardson number increases, the power due to work forces  
 386 decreases and the thermal power in the channel increases.  $\mathcal{J}_1$  is reduced by  
 387 a factor 1.64 and  $\mathcal{J}_2$  is reduced by a factor 1.51 (Table 2) for Ri = 100.  
 388 When we compare  $\mathcal{J}_1$  to its value without optimization  $\mathcal{J}_1^{\text{Ref}}$ , we notice  
 389 that sometimes the optimization algorithm added material which contributes  
 390 to rising friction forces and pressure losses as long as the heat dissipation  
 391 increases. Hence, for the case Ri = 200,  $\mathcal{J}_1$  is reduced by a factor 1.13



(a)  $Ri = 100$   
 $\omega = 0.5$



(b)  $Ri = 200$   
 $\omega = 0.85$



(c)  $Ri = 400$   
 $\omega = 0.15$

Figure 5: Adimensional vertical velocity field at various  $Ri$

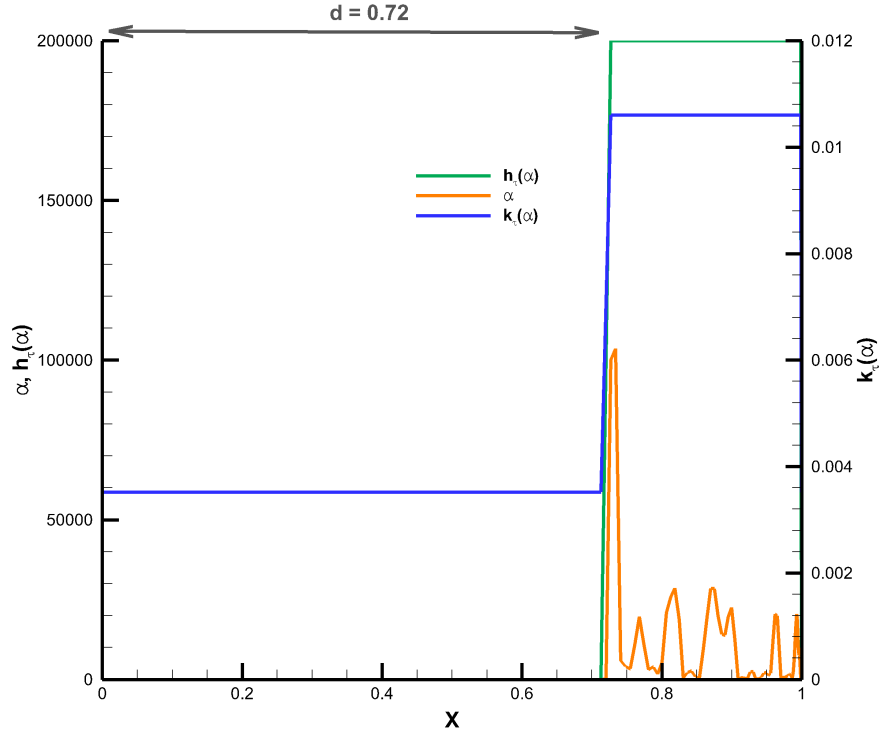


Figure 6:  $\alpha$ ,  $h_t(\alpha)$  and  $k_t(\alpha)$  at the end section of the channel for  $Ri = 100$  - annotation  $d$  is used for the width of the flow section

392 while  $\mathcal{J}_2$  is increased by a factor 0.46. On the contrary, for the case  $Ri =$   
 393 400,  $\mathcal{J}_1$  is increased by a factor 0.26 while  $\mathcal{J}_2$  is reduced by a factor 0.64.  
 394 These cases illustrated that our algorithm enables to add material in the  
 395 channel in order to contribute to one or other cost functions according to the  
 396 weighted coefficient  $\omega$ . Hence, for the case  $Ri = 200$ , we chose to prioritize  
 397 the minimization of mechanical power with  $\omega = 0.85$ . For the case  $Ri = 400$ ,  
 398 we chose to prioritize the maximization of heat transfer with  $\omega = 0.15$ . We  
 399 can conclude that the algorithm succeeds to minimize/maximize one or other

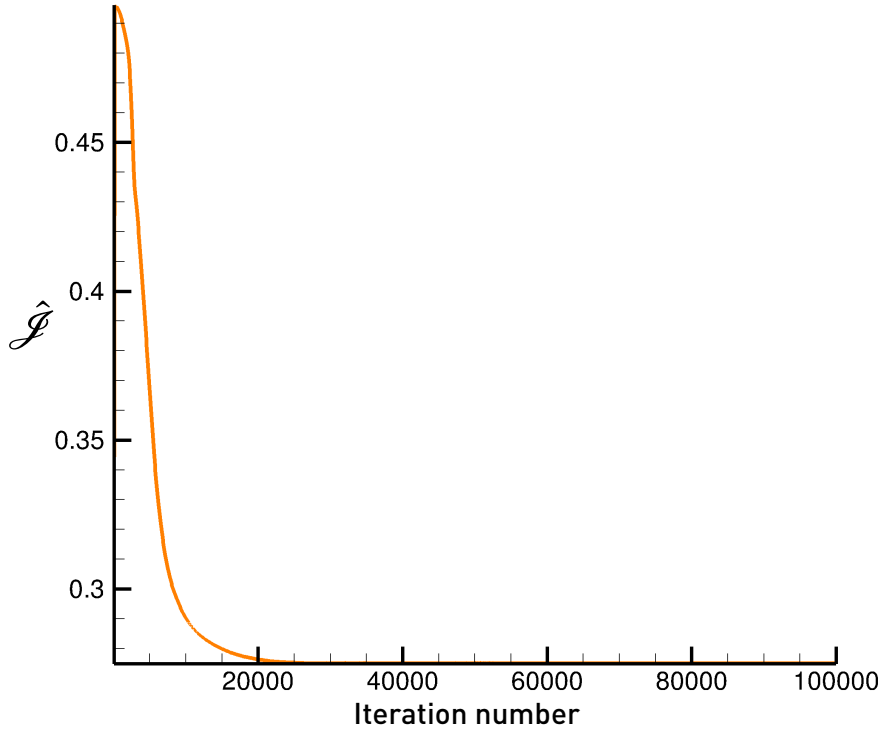


Figure 7: Evolution of  $\hat{\mathcal{J}}$  over iterations -  $\text{Ri} = 100, \omega = 0.5$

400 cost functions by adding material without penalizing too much the other.

401 *5.2. Comparison with classical functions of literature (Eq. 4) and (Eq. 5)*

402 In this section, we compare optimization results obtained with our cost  
 403 functions to those obtained with classical cost functions referenced in the  
 404 literature, i.e those defined by (Eq. 4) and (Eq. 5). First of all, Figure 11  
 405 shows different snapshot of optimized designs obtained over iterations with  
 406 classical cost functions (4) and (5). We stop the computation at iteration  
 407 number 187500. We notice that our algorithm has a tendency to fill up the

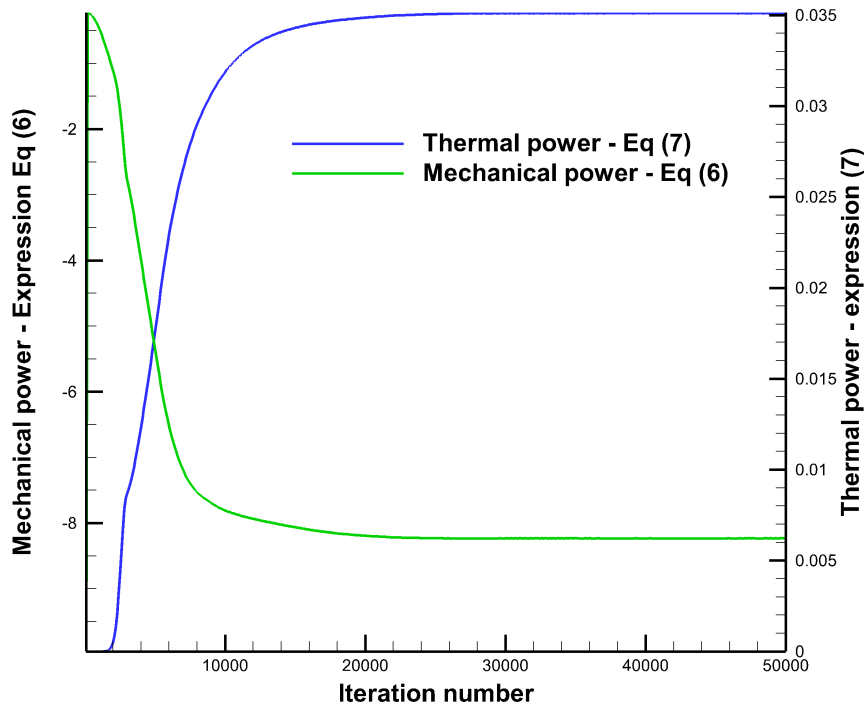


Figure 8: Evolution of thermal power and mechanical power over iterations -  $Ri = 100, \omega = 0.5$

408 channel with material before suppresses it in order to achieve the goal defined  
 409 by the classical cost functions. In the same way, Figure 9 shows different  
 410 snapshots of optimized designs over iterations with the objective functions  
 411 that we propose in this paper. We obtain the final optimized design at  
 412 iteration number 84000, which is faster compared to the previous simulation.  
 413 Ramalingom et al. [24] have used the same algorithm with the classical cost  
 414 functions to deal with cases where  $Ri = 2.8$ . When Richardson number is more  
 415 important (set to 100), the various designs obtained over iterations with these

	$\theta_{bulk}$	$Nu_2(3H/2)$
$Ri = 100$	0.027	11.86
$Ri = 200$	0.034	12.99
$Ri = 400$	0.039	15.06

Table 1: Nusselt number and adimensional bulk temperature at the end of the hot plate for various Richardson numbers

	Ri = 100	Ri = 200	Ri = 400
$\mathcal{J}_{1ref}/\mathcal{J}_1$	1.64	1.13	0.26
$\mathcal{J}_{2ref}/\mathcal{J}_2$	1.51	0.46	0.64

Table 2: Reduction factor of cost functions - ref corresponds to the value of cost functions without optimization

416 classical cost functions demonstrate that they are not appropriate to deal  
417 with heat transfer problem dominated by natural convection. Cost functions  
418 that dissociate pressure and temperature to the mass flow rate by considering  
419 average quantities essentially give stable optimized results. Moreover, we  
420 observe that the algorithm adds material just at the right plate on the top,  
421 this strategy is sufficient to prevent the fluid from re-entering at the top-end  
422 of the channel. Second, the channel is filled up at 45.03% with classical cost  
423 functions, while it is filled up at 4.9% with our cost functions. So, the new  
424 expressions of mechanical and thermal power give optimized designs with  
425 less material. Finally, when we enlarge the top end of the optimized designs  
426 and we compare both in Figure 10, we can see that the new expressions  
427 of objective functions allow a best connectivity between solid elements. No

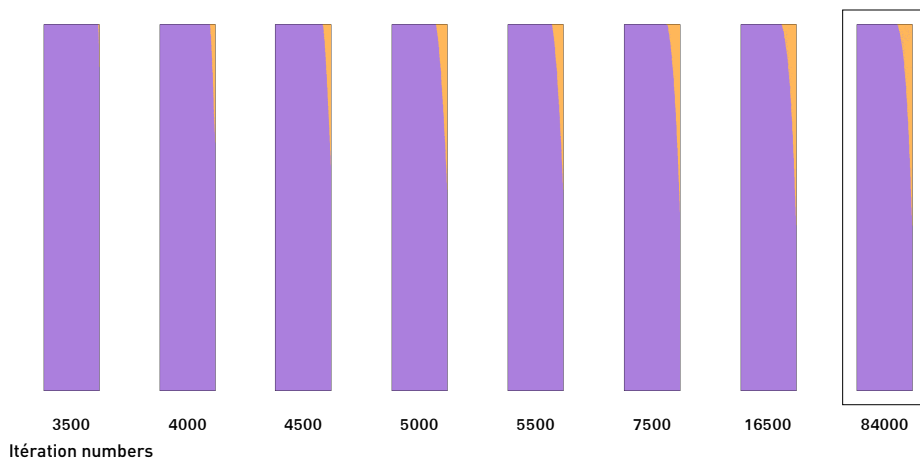


Figure 9: Designs obtained over iterations with functional objectives defined in this paper

428 isolated material is added in the channel as encountered by some authors  
 429 [41, 15, 12, 13] in the literature. Hence, that contributes to diminishing  
 430 the first objective function, i.e pressure losses in the channel. So, for this  
 431 configuration case of the channel, i.e. where the fluid flow moves essentially  
 432 by natural convection, the classical cost functions of the literature seem to be  
 433 inappropriate. With our new expressions of mechanical and thermal power,  
 434 we obtain an optimized design in less time of computation and with less  
 435 quantity of material. Moreover, connectivity in solid region is better.

## 436 6. Conclusion

437 An optimization problem considering both pressure drop minimization  
 438 and heat transfer maximization in the asymmetrically heated channel has  
 439 been examined. The problem is handled in natural convection with sev-  
 440 eral values of Richardson number taken in  $\{100, 200, 400\}$ . First of all, two  
 441 objective functions are investigated representing the work of forces for the

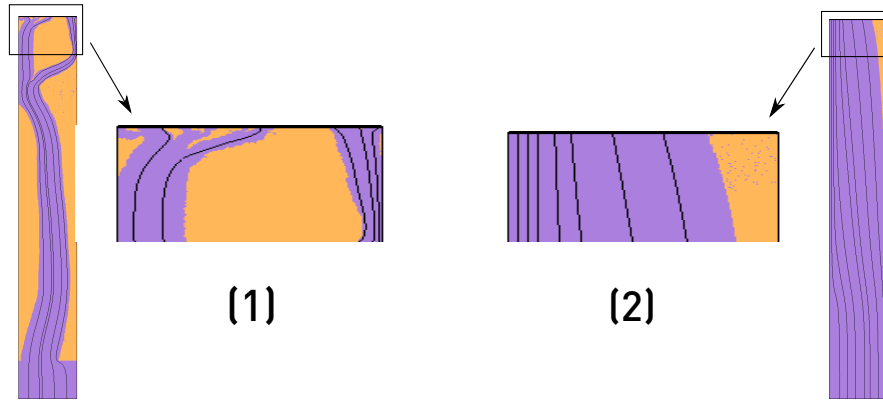


Figure 10: Comparison of solid regions at the end of the channel for classical cost functions of literature (1) and cost functions in this paper (2)

442 mechanical power and heat exchanges with the thermal power. In accordance  
 443 with the physical problem considered, a weighted coefficient is chosen for the  
 444 combined cost function. These functions allow to obtain optimal designs and  
 445 they are relatively reduced in accordance with the weight affected to each of  
 446 them. For Richardson number equal to 100, optimization results obtained  
 447 with cost functions proposed in this paper are compared to those obtained  
 448 with cost functions classically used in the literature. Several conclusions have  
 449 been drawn. First of all, the reversal flow in the channel is suppressed at  
 450 the end of the optimization. That contributes to reducing pressure losses in  
 451 the channel. Then, the new expressions of cost functions avoid the use of  
 452 filter techniques as no checkerboards pattern are observed. The values of cost  
 453 functions converge asymptotically over iterations with the new expressions  
 454 of mechanical and thermal powers, contrarily to those used in the litera-  
 455 ture. This approach that consists of dissociating quantities in the expression  
 456 of cost functions by considering average quantities is well adapted to natu-

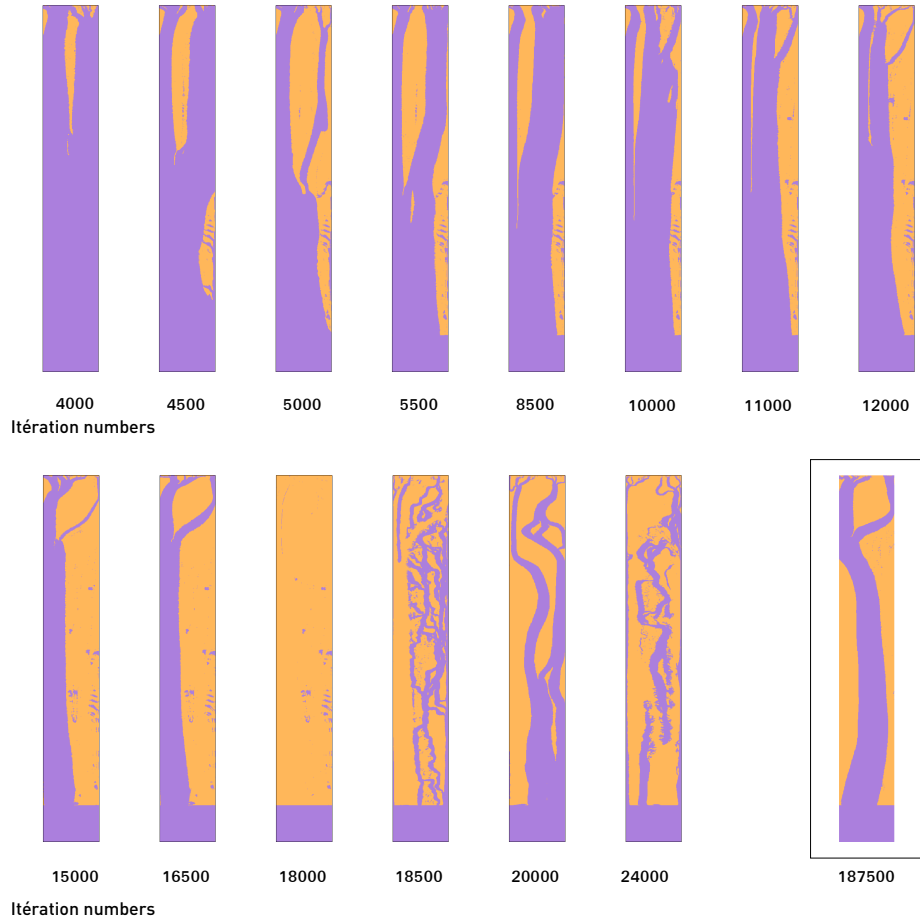


Figure 11: Designs obtained over iterations with cost functions defined in this paper

457 ral convection phenomena. Moreover, the obtained designs with these new  
 458 costs functions show a better connectivity in the solid region, contrarily to  
 459 the design obtained with classical cost functions. Concerning the fluid-solid  
 460 boundary, they are well-defined during the optimization process thanks to  
 461 two sigmoid functions used for the interpolation of both the design variable  
 462 and the effective diffusivity. Finally, the optimization algorithm is able to  
 463 increase thermal exchanges while maintaining the pressure losses due to fric-

464 tion, thanks to the combined objective functions used. Thermal exchanges  
465 are evaluated by the calculation of Nusselt number based on the bulk tem-  
466 perature. They are more important with the obtained optimized designs and  
467 increase with Richardson number values. In conclusion, this study highlights  
468 the importance of the expression of cost functions in a topology optimiza-  
469 tion problem, dominated by natural convection forces. The influence of the  
470 Richardson is observed on the quantity of material added in the optimized  
471 channel. As future work, we suggest a more complete heat and mass transfer  
472 model might be considered, as pure natural convection problems and radia-  
473 tion problems.

474 **Acknowledgements**

475 Computations have been performed on the University of Reunion Island  
476 supercomputer facility.

477 **References**

- 478 [1] M. P. Bendsøe, N. Kikuchi, Generating optimal topologies in structural  
479 design using a homogenization method, *Computer methods in applied  
480 mechanics and engineering* 71 (2) (1988) 197–224.
- 481 [2] O. Sigmund, K. Maute, *Topology optimization approaches*, 2013.
- 482 [3] H. A. Eschenauer, N. Olhoff, Topology optimization of continuum struc-  
483 tures: a review, *Applied Mechanics Reviews* 54 (4) (2001) 331–390.
- 484 [4] Q. Q. Liang, Performance-based optimization: a review, *Advances in  
485 Structural Engineering* 10 (6) (2007) 739–753.
- 486 [5] B. Hassani, E. Hinton, A review of homogenization and topology  
487 optimization II analytical and numerical solution of homogenization equa-  
488 tions, *Computers & structures* 69 (6) (1998) 719–738.
- 489 [6] B. Hassani, E. Hinton, A review of homogenization and topology op-  
490 timization I homogenization theory for media with periodic structure,  
491 *Computers & Structures* 69 (6) (1998) 707–717.
- 492 [7] B. Hassani, E. Hinton, A review of homogenization and topology opti-  
493 mization III topology optimization using optimality criteria, *Computers  
494 & structures* 69 (6) (1998) 739–756.

- 495 [8] M. Y. Wang, X. Wang, D. Guo, A level set method for structural topol-  
496 ogy optimization, *Computer methods in applied mechanics and engi-*  
497 *neering* 192 (1-2) (2003) 227–246.
- 498 [9] T. Borrvall, J. Petersson, Topology optimization of fluids in Stokes flow,  
499 *International journal for numerical methods in fluids* 41 (1) (2003) 77–  
500 107.
- 501 [10] T. Dbouk, A review about the engineering design of optimal heat trans-  
502 fer systems using topology optimization, *Applied Thermal Engineering*  
503 112 (2017) 841–854.
- 504 [11] C. Othmer, Adjoint methods for car aerodynamics, *Journal of Mathe-*  
505 *matics in Industry* 4 (1) (2014) 6.
- 506 [12] G. Marck, M. Nemer, J.-L. Harion, Topology optimization of heat and  
507 mass transfer problems: laminar flow, *Numerical Heat Transfer, Part B:*  
508 *Fundamentals* 63 (6) (2013) 508–539.
- 509 [13] J. Alexandersen, N. Aage, C. S. Andreasen, O. Sigmund, Topology op-  
510 timisation for natural convection problems, *International Journal for*  
511 *Numerical Methods in Fluids* 76 (10) (2014) 699–721.
- 512 [14] A. A. Koga, E. C. C. Lopes, H. F. V. Nova, C. R. de Lima, E. C. N.  
513 Silva, Development of heat sink device by using topology optimization,  
514 *International Journal of Heat and Mass Transfer* 64 (2013) 759–772.
- 515 [15] T. E. Bruns, Topology optimization of convection-dominated, steady-  
516 state heat transfer problems, *International Journal of Heat and Mass*  
517 *Transfer* 50 (15-16) (2007) 2859–2873.

- 518 [16] G. H. Yoon, Topological design of heat dissipating structure with forced  
519 convective heat transfer, *Journal of Mechanical Science and Technology*  
520 24 (6) (2010) 1225–1233.
- 521 [17] E. Kontoleonos, E. Papoutsis-Kiachagias, A. Zymaris, D. Papadim-  
522 itriou, K. Giannakoglou, Adjoint-based constrained topology optimiza-  
523 tion for viscous flows, including heat transfer, *Engineering Optimization*  
524 45 (8) (2013) 941–961.
- 525 [18] E. M. Papoutsis-Kiachagias, K. C. Giannakoglou, Continuous adjoint  
526 methods for turbulent flows, applied to shape and topology optimiza-  
527 tion: Industrial applications, *Archives of Computational Methods in*  
528 *Engineering* 23 (2) (2016) 255–299.
- 529 [19] C. Othmer, A continuous adjoint formulation for the computation of  
530 topological and surface sensitivities of ducted flows, *International Jour-  
531 nal for Numerical Methods in Fluids* 58 (8) (2008) 861–877.
- 532 [20] A. Bastide, P.-H. Cocquet, D. Ramalingom, Penalization model for  
533 navier-stokes-darcy equation with application to porosity-oriented topol-  
534 ogy optimization, *Mathematical Models and Methods in Applied Sci-  
535 ences* 0 (0) (2017) 1–32.
- 536 [21] Z.-X. Tong, M.-J. Li, J.-J. Yan, W.-Q. Tao, Optimizing thermal con-  
537 ductivity distribution for heat conduction problems with different op-  
538 timization objectives, *International Journal of Heat and Mass Transfer*  
539 119 (2018) 343–354.

- 540 [22] C. Othmer, T. Kaminski, R. Giering, Computation of topological sensi-  
541 tivities in fluid dynamics: cost function versatility, in: ECCOMAS CFD  
542 2006: Proceedings of the European Conference on Computational Fluid  
543 Dynamics, Egmond aan Zee, The Netherlands, September 5-8, 2006,  
544 Citeseer, 1–12, 2006.
- 545 [23] M. Zhou, G. Rozvany, The COC algorithm, Part II: topological, geomet-  
546 rical and generalized shape optimization, *Computer Methods in Applied  
547 Mechanics and Engineering* 89 (1-3) (1991) 309–336.
- 548 [24] D. Ramalingom, P.-H. Cocquet, A. Bastide, A new interpolation tech-  
549 nique to deal with fluid-porous media interfaces for topology optimiza-  
550 tion of heat transfer, *Computers & Fluids* 168 (2017) 144 – 158.
- 551 [25] F. M. White, *Fluid Mechanics Fourth Edition*, 2017.
- 552 [26] T. L. Bergman, F. P. Incropera, A. S. Lavine, D. P. DeWitt, *Introduction  
553 to heat transfer*, John Wiley & Sons, 2011.
- 554 [27] P. Coffin, K. Maute, Level set topology optimization of cooling and heat-  
555 ing devices using a simplified convection model, *Structural and multi-  
556 disciplinary optimization* 53 (5) (2016) 985–1003.
- 557 [28] B. S. Lazarov, O. Sigmund, Filters in topology optimization based on  
558 Helmholtz-type differential equations, *International Journal for Numer-  
559 ical Methods in Engineering* 86 (6) (2011) 765–781.
- 560 [29] T. Bruns, A reevaluation of the SIMP method with filtering and an  
561 alternative formulation for solid–void topology optimization, *Structural  
562 and Multidisciplinary Optimization* 30 (6) (2005) 428–436.

- 563 [30] K. Lee, Topology optimization of convective cooling system designs,  
564 Ph.D. thesis, University of Michigan, 2012.
- 565 [31] J. Alexandersen, C. S. Andreasen, N. Aage, B. S. Lazarov, O. Sigmund,  
566 Topology optimisation for coupled convection problems, in: 10th world  
567 Congress on structural and multidisciplinary optimization, Orlando, 19–  
568 24, 2013.
- 569 [32] O. Sigmund, Morphology-based black and white filters for topology opti-  
570 mization, *Structural and Multidisciplinary Optimization* 33 (4-5) (2007)  
571 401–424.
- 572 [33] E. Bacharoudis, M. G. Vrachopoulos, M. K. Koukou, D. Margaris, A. E.  
573 Filios, S. A. Mavrommatis, Study of the natural convection phenomena  
574 inside a wall solar chimney with one wall adiabatic and one wall under  
575 a heat flux, *Applied Thermal Engineering* 27 (13) (2007) 2266–2275.
- 576 [34] F. Incropera, Convection heat transfer in electronic equipment cooling,  
577 *Journal of heat transfer* 110 (4b) (1988) 1097–1111.
- 578 [35] R. B. Yedder, E. Bilgen, Natural convection and conduction in Trombe  
579 wall systems, *International Journal of Heat and Mass Transfer* 34 (4-5)  
580 (1991) 1237–1248.
- 581 [36] B. F. Balunov, A. Babykin, R. A. Rybin, V. A. Krylov, V. N. Tanchuk,  
582 S. A. Grigor'ev, Heat transfer at mixed convection in vertical and in-  
583 clined flat channels of the vacuum chamber of the iter international  
584 thermonuclear reactor, *High temperature* 42 (1) (2004) 126–133.

- 585 [37] R. C. Martinelli, L. M. K. Boelter, The Analytical Prediction of Super-  
586 posed Free and Forced Viscous Convection in a Vertical Pipe, by RC  
587 Martinelli and LMK Boelter..., University of California Press, 1942.
- 588 [38] J. Jackson, M. Cotton, B. Axcell, Studies of mixed convection in vertical  
589 tubes, International journal of heat and fluid flow 10 (1) (1989) 2–15.
- 590 [39] J. Bodoia, J. Osterle, The development of free convection between  
591 heated vertical plates, Journal of Heat Transfer 84 (1) (1962) 40–43.
- 592 [40] W. Elenbaas, Heat dissipation of parallel plates by free convection, Phys-  
593 ica 9 (1) (1942) 1–28.
- 594 [41] G. Ho Yoon, Y. Young Kim, The element connectivity parameterization  
595 formulation for the topology design optimization of multiphysics sys-  
596 tems, International journal for numerical methods in engineering 64 (12)  
597 (2005) 1649–1677.
- 598 [42] G. Desrayaud, E. Chénier, A. Joulin, A. Bastide, B. Brangeon, J. Cal-  
599 tagirone, Y. Cherif, R. Eymard, C. Garnier, S. Giroux-Julien, et al.,  
600 Benchmark solutions for natural convection flows in vertical channels  
601 submitted to different open boundary conditions, International journal  
602 of thermal sciences 72 (2013) 18–33.
- 603 [43] D. Ramalingom, P.-H. Cocquet, A. Bastide, Numerical study of nat-  
604 ural convection in asymmetrically heated channel considering thermal  
605 stratification and surface radiation, Numerical Heat Transfer, Part A:  
606 Applications 72 (9) (2017) 681–696.

- 607 [44] T. W. Athan, P. Y. Papalambros, A note on weighted criteria methods  
608 for compromise solutions in multi-objective optimization, 1996.
- 609 [45] A. Messac, C. Puemi-Sukam, E. Melachrinoudis, Aggregate objective  
610 functions and Pareto frontiers: required relationships and practical im-  
611 plications, *Optimization and Engineering* 1 (2) (2000) 171–188.
- 612 [46] J. K. Guest, J. H. Prévost, T. Belytschko, Achieving minimum length  
613 scale in topology optimization using nodal design variables and projec-  
614 tion functions, *International journal for numerical methods in engineer-*  
615 *ing* 61 (2) (2004) 238–254.
- 616 [47] X. Zhao, M. Zhou, O. Sigmund, C. S. Andreasen, A poor mans ap-  
617 proach to topology optimization of cooling channels based on a Darcy  
618 flow model, *International Journal of Heat and Mass Transfer* 116 (2018)  
619 1108–1123.
- 620 [48] H. Everett III, Generalized Lagrange multiplier method for solving prob-  
621 lems of optimum allocation of resources, *Operations research* 11 (3)  
622 (1963) 399–417, ISSN 0030-364X.
- 623 [49] G. H. W. Et al., A tensorial approach to computational continuum me-  
624 chanics using object- oriented techniques, *Computers in physics* 12.6  
625 (1998) 620–631.
- 626 [50] R. Li, M. Bousetta, E. Chénier, G. Lauriat, Effect of surface radiation  
627 on natural convective flows and onset of flow reversal in asymmetrically  
628 heated vertical channels, *International journal of thermal sciences* 65  
629 (2013) 9–27.

630 [51] S. Kreissl, K. Maute, Levelset based fluid topology optimization using  
631 the extended finite element method, *Structural and Multidisciplinary*  
632 *Optimization* 46 (3) (2012) 311–326.